Improved reference tracts for unsupervised brain white matter tractography

Improved reference tracts for unsupervised brain white matter tractography

Susana Muñoz Maniega[1,2], Mark E. Bastin[1,2], Ian J. Deary[2,3], Joanna M. Wardlaw[1,2] and Jonathan D. Clayden[4]

[1]Department of Neuroimaging Sciences, University of Edinburgh, UK
[2]Centre for Cognitive Ageing and Cognitive Epidemiology, University of Edinburgh, UK
[3]Department of Psychology, University of Edinburgh, UK
[4] Great Ormond Street Institute of Child Health, University College London, UK

Abstract. Neighbourhood tractography aims to automatically segment equivalent brain white matter tracts from diffusion magnetic resonance imaging (dMRI) data in different subjects by using a "reference tract" as a prior for the shape and length of each tract of interest. In the current work we present a means of improving the technique by using references tracts derived from dMRI data acquired from 80 healthy volunteers aged 25–64 years. The reference tracts were tested on the segmentation of 16 major white matter tracts in 50 healthy older people, aged 71.8 (±0.4) years. We found that data-generated reference tracts improved the automatic white matter tract segmentations compared to results from atlas-generated reference tracts. We also obtained higher percentages of visually acceptable segmented tracts and lower variation in water diffusion parameters using this approach.

Keywords: MRI; Brain; White matter; Unsupervised segmentation; Tractography.

1 Introduction

Tractography uses dMRI data to reconstruct in vivo the white matter connections within the brain [1]. Clinical applications of tractography typically involve group analysis, where tract characteristics are examined across a patient group of interest, or compared to a matched control group. In these instances, sources of nuisance variance within and between groups—and in particular any variability introduced by the tract segmentation method—need to be kept to a minimum to facilitate detection of true biological differences and avoid spurious findings. Probabilistic neighbourhood tractography (PNT) aims to reduce operator interaction, and therefore any potential variability induced by it, during the tract segmentation process. PNT automatically

segments the same white matter fasciculus in different subjects by scoring the similarity between a predefined "reference tract" and a group of candidate tracts generated with different initial seed points within a neighbourhood [2, 3]. Other automated tract segmentation tools informed by prior information have also been developed [4] Reference tracts can be generated directly from dMRI data, or from an atlas or similar reference point. In either case, the underlying reference dataset should be representative of the population. A suitably large and diverse "training" dataset is subsequently used to capture the variability typically observed around each reference tract. However, this set of training data should generally be kept separate from the data that will be used for hypothesis testing, to prevent any potential bias during analysis. To avoid use of valuable testing data in the creation of reference tracts, and for consistency across studies, a set of reference tracts has been previously derived from a white matter atlas, which is independent of all new subject data acquired [5, 6]. These atlas-based reference tracts improved significantly the results from PNT, however a small a proportion of the segmented tracts still needed excluding after visual inspection [7].
In the current work, we are proposing a new set of reference tracts directly derived from dMRI data acquired from a large group of healthy volunteers with a wide age range, so as to capture the variability due to age. We then test these new reference tracts on a different set of healthy older volunteers.

2 Methods

2.1 Participants

Training data. The reference and training data consisted of brain dMRI from 80 clinically normal, right-handed, healthy volunteers (40 males, 40 females) aged 25–64 years. All participants gave written informed consent. Health status was assessed using medical questionnaires and all structural MRI scans were reported by a fully qualified neuroradiologist. More details can be found in previous publications [8].

Testing data. The testing data consisted of brain dMRI data from 50 healthy, community-dwelling older participants from the Lothian Birth

Cohort 1936 (LBC1936), all born in the same year, with average age 71.8 ± 0.4 years at the time of scanning. All participants gave written informed consent. More details of this cohort have been published previously [9].

2.2 MRI

All brain MRI data were acquired using the same GE Signa Horizon HDxt 1.5T clinical scanner (General Electric, Milwaukee, WI, USA) equipped with a self-shielding gradient set (33 mT/m maximum gradient strength) and manufacturer supplied eight-channel phased-array head coil. The same dMRI protocol was used for both training and testing data. The acquisition consisted of seven T_2-weighted (T2W; b=0 s/mm^2) and sets of diffusion-weighted (b=1000 s/mm^2) single-shot, spin-echo, echo-planar (EP) imaging volumes, acquired with diffusion gradients applied in 64 non-collinear directions [10] and 2 mm isotropic spatial resolution.

2.3 Image analysis

dMRI volumes were preprocessed using FSL tools (http://www.fmrib.ox.ac.uk/fsl) to extract the brain [11], remove bulk motion and correct eddy current induced distortions by registering all subsequent volumes to the first T2W EP volume [12]. The water self-diffusion tensor was calculated, and parametric maps of fractional anisotropy (FA) and mean diffusivity (MD) derived from its eigenvalues using DTIFIT.

2.4 Creation of reference tracts

We followed the standard reference tract construction steps for PNT in the TractoR software package v.2.1 for all reference datasets (http://www.tractor-mri.org.uk/reference-tracts#creating-custom-reference-tracts;[13]). Briefly, for each tract of interest, a seed point was chosen in standard space and registered linearly to each of the 80 training datasets. A cuboidal region of interest (ROI) was created in the 7×7×7 voxel neighbourhood around each of these original seeds in native space. A probabilistic tract was then created for each voxel in the neighbourhood with FA>0.2, using BEDPOSTx/PROBTRACKx as the

underlying tractography algorithm [14], with 2000 streamlines and a two-fibre model. All the tracts generated were reviewed visually, and for each dataset we manually chose the seed that produced the tract most closely representing the expected shape and length of the fasciculus of interest. In the cases where there was more than one potential candidate available, we chose the one generated from the seed closest to the centre of the neighbourhood, i.e. closest to the seed point selected originally in standard space.
We therefore obtained 80 representative training tracts for each tract of interest. Each of them was reduced to a single streamline by obtaining the spatial median [3], and then mapped into the standard MNI brain (with its corresponding seed point) by applying the reverse linear transformation. A reference tract was then created by obtaining the median seed point and median streamline from the 80 training tracts, and fitting a B-spline to it, with a distance between knots of approximately 6 mm. A maximum bending angle restriction of 90^{o} was also applied to avoid unrealistic 'twists' at the ends of the tracts, where uncertainty is larger.

2.5 Creation of matching models

The "matching model" describes typical deviations in shape and length that matching tract pathways make from the reference tract, using maximum likelihood estimation. The model for a tract of interest may be fitted in a supervised fashion by manually choosing a set of training tracts representing good matches to the reference [3], or following an unsupervised approach using an expectation-maximisation (EM) algorithm which will train the model and select at the same time the best segmentations from each dataset [2].
With the centroid reference tract created from the training data as explained above, the whole set of 80 training tracts were used to fit a matching model in a supervised fashion [3].
We then used an unsupervised approach in the 50 testing datasets (LBC1936), based on an EM algorithm, whereby the model was trained and applied iteratively using the same data [2]. Using this approach, a matching model was obtained from the testing data as well as the best candidate tract for each dataset. We therefore obtained two matching models for each tract of interest, one created from the 80 training

datasets (ages 25–64 years) and one created from the 50 testing datasets (age 71.8 ± 0.4 years).

2.6 Testing of reference tracts and matching models

The new reference tracts were used to segment the fasciculi of interest in the LBC1936 testing data with PNT by evaluating novel candidate tracts for plausibility against the model fitted to the training data and against the model created with the unsupervised approach in the own testing data. This allows us to test the influence of the matching model on the selection of candidate tracts in the testing data.

The unsupervised fitting process was also repeated using the reference tracts previously created from an atlas [6, 15], which are currently provided with the TractoR package. This allows the new data-based reference tracts to be compared with the previous atlas-based reference tracts.

We therefore obtained three segmentations for each fasciculus of interest for each testing dataset (LBC1936): (a) using a supervised matching model from the training dataset and the data-based reference tract, (b) using an unsupervised matching model from the testing LBC1936 dataset and the data-based reference tract, and (c) using an unsupervised matching model from the testing LBC1936 dataset and the atlas-based reference tract.

For all methods, an additional shape modelling-based approach was used to reject false positive streamlines from the final tracts [16]. The resulting segmented tracts were then visually assessed, blinded to the method used, and tracts were considered unacceptable if any significant portion of the tract (i.e. with high visitation count) ran in a direction different from that expected from anatomy, or if they were severely truncated or bent in an unrealistic angle.

Tract-averaged FA and MD values were then calculated in tracts that passed this visual quality check, weighting the values in each voxel by the streamline visitation count. To compare the three segmentations, the proportions of visually plausible tracts were recorded and the coefficients of variation (CV) of the mean FA and MD values extracted from the resulting tracts calculated and compared.

To obtain an impression of the relative importance of the reference tracts and the fitted model, the degree of agreement on the best-

matching candidate tract was assessed across the 50 LBC1936 testing datasets between the three methods

3 Results

3.1 Reference tracts

The data-based reference tracts were created for 16 main brain white matter fasciculi: the genu and splenium of the corpus callosum, the anterior thalamic radiations (ATR), the arcuate (Arc), uncinate (Unc), and inferior longitudinal fasciculi (ILF), the frontal and ventral cingula (Cing), and the corticospinal tract (CST), bilaterally. Figure 1 shows a representation of all the reference tracts created from the training data as a projection in a plane.

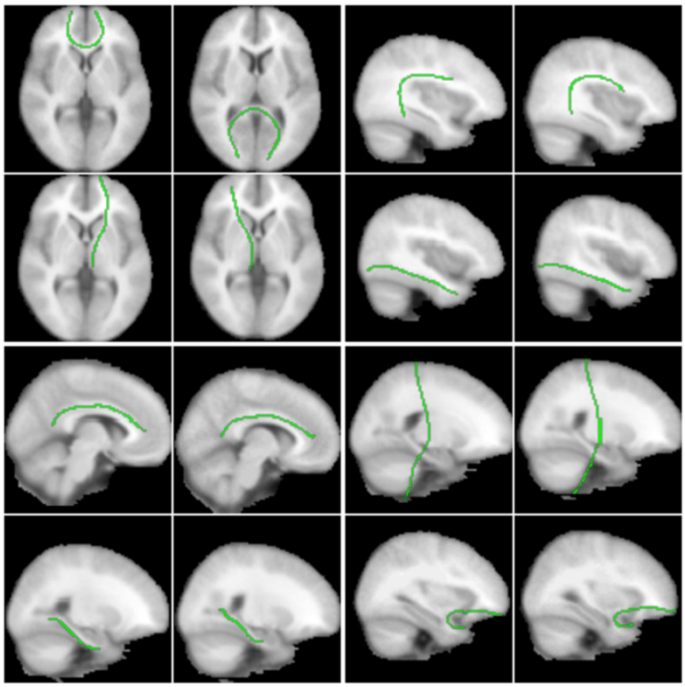

Fig. 1. 2D projections of the reference tracts created form the training data. From left to right and top to bottom: genu and splenium of the corpus callosum, left (L) and right (R) arcuate fasciculi, L and R anterior thalamic radiations, L and R inferior longitudinal fasciculi, L and R frontal cingula, L and R corticospinal tracts, L and R ventral cingula, and L and R uncinate fasciculi. Note: images are in radiological convention (left is shown on the right)

3.2 Testing of reference tracts and matching models

Visual assessments. The use of the data-based reference tracts improved the number of visually acceptable tracts when compared with the same segmentations created from the previous atlas-based reference tracts. Table 1 shows the percentage of successful segmentations for each white matter tract using each method.
When comparing tracts created with the same testing data model, the data-based reference tracts improved the consistency of the segmentations, with >92% of successful segmentations for all tracts. By contrast, atlas-based reference tracts had a lower average performance, particularly due to the poor performance segmenting the ATR, bilaterally, where only 32 and 76% of the cases could be segmented successfully.
When comparing the two models, both perform well, with an average of >98% visually plausible tracts, suggesting that a model can be trained in a separate dataset and still successfully segment the tracts in the testing (LBC1936) data.

Table 1. Proportion of segmented tracts visually acceptable when using two different matching models and each set of reference tracts as priors.

Reference tracts	*Data-based*		*Atlas-based*
Model trained on	*Training data*	*Testing data*	
Genu	100.0%	100.0%	96.0%
Splenium	98.0%	96.0%	98.0%
LArc	100.0%	100.0%	98.0%
RArc	96.0%	96.0%	94.0%
LATR	100.0%	100.0%	32.0%
RATR	96.0%	100.0%	76.0%
LCing	98.0%	98.0%	100.0%
RCing	98.0%	92.0%	98.0%
LCing_ventral	98.0%	100.0%	98.0%
RCing_ventral	94.0%	98.0%	100.0%
LILF	100.0%	100.0%	100.0%
RILF	100.0%	100.0%	100.0%
LUnc	96.0%	92.0%	88.0%
RUnc	100.0%	100.0%	100.0%
LCST	100.0%	98.0%	100.0%
RCST	100.0%	100.0%	100.0%
Mean	*98.3%*	*98.1%*	*92.4%*

Figure 2 shows the group maps created by overlaying the segmented tracts from the 50 older age volunteer LBC1936 testing data set into the standard brain as maximum intensity projections. These images show that the segmentations obtained from the two sets of reference tracts are similar, except for the left and right ATR, where many of the

segmentations using the atlas-based reference followed the wrong path, thereby failing the visual check. Some small differences are, however, obvious in other tracts, specifically regarding their lengths. In particular, the segmentations of the corpus callosum genu, the arcuate fasciculi and the ventral cingula were longer when using the new data-based reference tracts, with more of the tract included in the segmentation.

The group maps from tracts generated with each training model showed that the choice of training model had a modest effect on the segmented tracts.

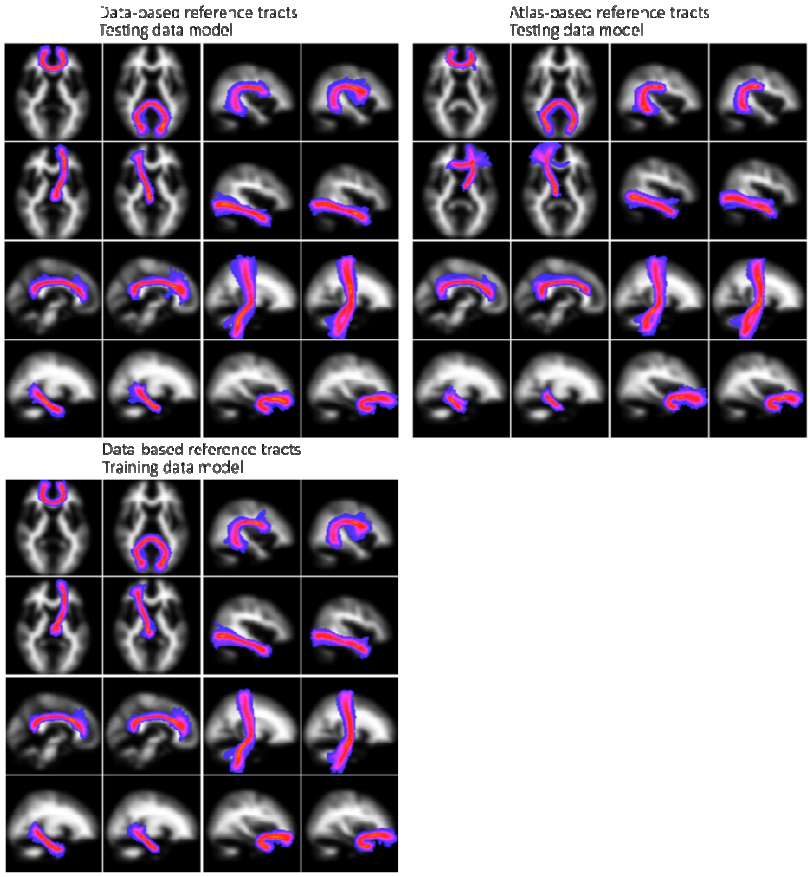

Fig. 2. Group maps projections for the 16 tracts of interest segmented using the atlas-based (left) and data-based (right) reference tracts. Top row used a matching model trained in the testing data, and the bottom row used a model trained in the training data. Colour scale represents the voxel visitation frequency, from 1 (dark blue) to 50 (yellow). Maps are projected into the plane of the voxel with maximum visitation value.

FA and MD variability. Table 2 shows the mean values and CV of FA and MD, measured along the tracts extracted by the three methods. One-way analysis of variance (ANOVA) tests, corrected for multiple comparisons, showed that the parameters measured in tracts generated by each method were generally not significantly different. Only the corpus callosum splenium, the RATR and RCST produced significantly different mean parameters. Without multiple comparison correction, genu (FA), LCing (FA) and LCST (FA and MD) also became significant. However, for both the FA and MD, the variation across the 50 LBC1936 datasets is lower for most tracts when generated with the data-based reference tracts.

Table 2. Averaged values of fractional anisotropy (FA) and mean diffusivity (MD) measured along the tracts segmented with two different matching models, and atlas-based or data-based reference tracts as priors in 50 older age volunteers. The coefficients of variation (CV) for each parameter are shown in the shaded columns. Bold type indicates that the mean parameters were significantly different ($p<0.05$) between the tracts created with each method (One-way ANOVA after Bonferroni-Holm adjustment for multiple comparisons across tracts).

	FA						***MD ($10^{-6}mm^2/s$)***					
Reference	***Atlas-based***		***Data-based***				***Atlas-based***		***Data-based***			
Model training	***Testing data***				***Training data***		***Testing data***				***Training data***	
	Mean (sd)	***CV***	***Mean (sd)***	***CV***	***Mean (sd)***	***CV***	***Mean (sd)***	***CV***	***Mean (sd)***	***CV***	***Mean (sd)***	***CV***
Genu	0.41 (0.05)	0.11	0.39 (0.05)	0.12	0.39 (0.05)	0.12	776.91 (65.59)	0.08	799.20 (75.46)	0.09	799.85 (74.59)	0.09
Splenium	**0.45 (0.09)**	0.20	**0.52 (0.06)**	0.12	**0.51 (0.08)**	0.15	**1117.26 (220.22)**	0.20	**807.61 (108.59)**	0.13	**837.77 (162.71)**	0.19
LArc	0.46 (0.05)	0.10	0.45 (0.04)	0.09	0.45 (0.04)	0.10	663.30 (49.21)	0.07	661.30 (49.26)	0.07	659.82 (49.73)	0.08
RArc	0.43 (0.05)	0.12	0.42 (0.04)	0.10	0.43 (0.04)	0.09	646.56 (55.00)	0.09	645.36 (48.93)	0.08	644.13 (45.30)	0.07
LATR	0.34 (0.05)	0.14	0.34 (0.03)	0.10	0.34 (0.03)	0.10	757.89 (81.23)	0.11	755.39 (60.94)	0.08	746.41 (60.30)	0.08
RATR	**0.35 (0.04)**	0.10	**0.36 (0.03)**	0.08	**0.33 (0.04)**	0.12	**747.07 (54.08)**	0.07	**704.05 (50.40)**	0.07	**766.81 (74.85)**	0.10
LCing	0.45 (0.05)	0.12	0.46 (0.06)	0.12	0.46 (0.06)	0.12	647.29 (51.00)	0.08	638.39 (45.15)	0.07	640.95 (47.46)	0.07
RCing	0.42 (0.06)	0.13	0.43 (0.04)	0.10	0.42 (0.05)	0.11	619.92 (36.16)	0.06	626.56 (36.03)	0.06	630.97 (33.82)	0.05
LCing_ventral	0.32 (0.06)	0.19	0.29 (0.04)	0.12	0.29 (0.04)	0.12	752.54 (155.54)	0.21	728.86 (62.50)	0.09	733.07 (69.52)	0.09
RCing_ventral	0.30 (0.06)	0.20	0.30 (0.05)	0.15	0.29 (0.04)	0.14	760.68 (95.07)	0.12	748.37 (79.00)	0.11	748.73 (88.67)	0.12
LILF	0.42 (0.05)	0.12	0.41 (0.05)	0.12	0.40 (0.05)	0.12	740.50 (75.45)	0.10	752.41 (67.06)	0.09	745.86 (61.13)	0.08
RILF	0.39 (0.05)	0.14	0.40 (0.04)	0.11	0.38 (0.05)	0.12	788.00 (142.54)	0.18	750.31 (83.70)	0.11	755.39 (87.47)	0.12
LUnc	0.34 (0.03)	0.10	0.33 (0.03)	0.10	0.34 (0.04)	0.11	767.04 (53.54)	0.07	767.63 (60.41)	0.08	764.88 (60.65)	0.08
RUnc	0.33 (0.03)	0.10	0.33 (0.03)	0.10	0.33 (0.04)	0.11	756.22 (41.27)	0.05	758.75 (41.27)	0.05	754.75 (41.77)	0.06
LCST	0.48 (0.03)	0.07	0.46 (0.04)	0.08	0.46 (0.04)	0.08	655.47 (36.72)	0.06	672.26 (37.18)	0.06	675.52 (38.65)	0.06
RCST	0.49 (0.03)	0.07	0.49 (0.03)	0.07	0.50 (0.04)	0.07	**653.82 (32.72)**	0.05	**676.03 (32.36)**	0.05	**676.37 (31.99)**	0.05
Mean	*0.40 (0.06)*	*0.13*	*0.40 (0.07)*	*0.10*	*0.40 (0.07)*	*0.11*	*740.65 (115.51)*	*0.10*	*718.28 (58.64)*	*0.08*	*723.83 (61.36)*	*0.09*

Comparison between fitted models. The source of training data used to fit the model appeared to be less influential than the choice of reference tract. Models trained with the separate training data or with the testing data (in the unsupervised framework), but with the reference tracts in common, resulted in agreement on the best candidate tract in an average of 39% of subjects. By contrast, the two models fitted in an unsupervised fashion on the same testing data (LBC1936), but with different reference tracts, agreed only 9% of the time.

4 Discussion

The reference tract represents the "matching" target for PNT automatic segmentation, and it is therefore crucial that this prior epitomises the topological characteristics of the fasciculus of interest correctly. Using a large group of healthy volunteers, with a wide age range, we were able to capture the variability in tract topology better. Our results showed that the results from PNT can be improved, even when the testing data corresponds to an age group outside the age range used during training to generate the reference tracts or the matching models (72 vs 25–64 years old). We also demonstrated that the source of training data used to fit the model was less influential than the choice of reference tract, and that matching models previously fitted in training data can be used to apply PNT in separate testing datasets. This enables the possibility of using PNT in small samples of testing data, where the number of datasets might not be large enough for fitting the matching model in an unsupervised fashion.

The large percentage of successful segmentations obtained in the older population (>98%) when using the new reference tracts suggests that these can be used as priors in different populations, and not just in a population matching the training data characteristics. Although the improvement is significant, is it still not sufficient to make manual checking of the segmented tracts entirely unnecessary, but this is true for most automated methods. Further tests would also be required to investigate whether these reference tracts would still be good priors to perform PNT segmentation in diseased populations with potentially large changes in brain topology, such as in the presence of tumours or

stroke, but preliminary work suggests that the general approach is robust to even quite substantial mass effects [17].

The most obvious improvement with the new reference tracts is the high success rate obtained for the ATR, indicating that the prior for this tract generated from real data is a much better representation of the ATR topology. Another improvement is the extraction of longer segments of some of the tracts of interest, such as the genu of the corpus callosum, the arcuate and the ventral cingulum, which arises due to the greater difficulty of inferring accurate pathways near the ends of tracts when using an atlas as the reference, leading to a shorter reference tract. The segmentation of a larger section of the genu projections into the frontal cortex (where FA tends to be lower than in the centre of the tract) could explain the slightly lower mean values of FA obtained for this tract when using the new reference tracts. There was also a very subtle shift in the overall position of the splenium of the corpus callosum, with the segmentations for this tract obtained with the atlas-based reference tract being generally closer to the boundary with the ventricles, while the data-based reference producing segmentations within the middle of this fasciculus. This is also reflected in the higher MD and lower FA of the atlas-based splenium, suggesting more partial volume averaging with cerebrospinal fluid from the ventricles.

There could be two main reasons for the differences in parameters measured with each method. Firstly, the atlas used to generate the previous references tracts was obtained using data from subjects with an average age of 29 ± 7.9 years [6], while the training data for the new priors had a wider age range of 25–65 years. The new reference tracts will therefore represent better the characteristics of the white matter in older age, and particularly the changes due to ageing such as atrophy and enlarged ventricles. This is reflected in the better segmentations, and in the change in the parameters measured, in the tracts running closer to the ventricles, such as the ATR, the CST, and the genu and splenium of the corpus callosum. Secondly, the native-space tractography data used for generating the reference tracts here is a much richer dataset than the subject-averaged tract probability maps that constitute the atlas.

The CVs in the parameters measured in the segmentations created from the new set of reference tracts are lower than those created from the atlas-based reference tracts, particularly for the splenium and the

ventral Cing. This suggests a lower variability introduced by the tract segmentation method, which should facilitate detection of true biological differences and avoid spurious findings.
In summary, we have created a new set of data-based reference tracts to be used as priors for PNT, which improved the segmentations of 16 tracts of interest. We have also demonstrated that the matching model could be fitted in separate training data, which will make the use of PNT in small testing datasets newly practicable.

Acknowledgements: LBC1936 was supported by the Age UK-funded Disconnected Mind project, with additional funding from the UK Medical Research Council (MR/M013111/1). MRI scanning for the training dataset was funded under NIH grant R01 EB004155-03. The scanning was performed at the Brain Research Imaging Centre, Edinburgh, part of Edinburgh Imaging (www.ed.ac.uk/clinical-sciences/edinburgh-imaging) and the SINAPSE Collaboration (Scottish Imaging Network, A Platform for Scientific Excellence, www.sinapse.ac.uk).

References

1. Tournier, J. D., Mori, S., Leemans, A.: Diffusion tensor imaging and beyond. Magn. Reson. Med., **65**, 1532–1556. (2011). doi:10.1002/mrm.22924
2. Clayden, J. D., Storkey, A. J., Muñoz Maniega, S., Bastin, M. E.: Reproducibility of tract segmentation between sessions using an unsupervised modelling-based approach. Neuroimage, **45**, 377–385. (2009). doi:10.1016/j.neuroimage.2008.12.010
3. Clayden, J. D., Storkey, A. J., Bastin, M. E.: A Probabilistic Model-Based Approach to Consistent White Matter Tract Segmentation. IEEE Trans. Med. Imaging, **26**, 1555–1561. (2007). doi:10.1109/TMI.2007.905826
4. Yendiki, A., Panneck, P., Srinivasan, P., Stevens, A., Zöllei, L., Augustinack, J., … Fischl, B.: Automated probabilistic reconstruction of white-matter pathways in health and disease using an atlas of the underlying anatomy. Front. Neuroinform., **5**, 23. (2011). doi:10.3389/fninf.2011.00023
5. Muñoz Maniega, S., Bastin, M. E., McIntosh, A. M., Lawrie, S. M., Clayden, J. D.: Atlas-based reference tracts improve automatic white matter segmentation with neighbourhood tractography. In ISMRM (Ed.), Proc. ISMRM 16th Sci. Meet. Exhib. (p. 3318). (2008).
6. Hua, K., Zhang, J., Wakana, S., Jiang, H., Li, X., Reich, D. S., … Mori, S.: Tract probability maps in stereotaxic spaces: analyses of white matter anatomy and tract-specific quantification. Neuroimage, **39**, 336–347. (2008). doi:10.1016/j.neuroimage.2007.07.053
7. Penke, L., Muñoz Maniega, S., Houlihan, L. M., Murray, C., Gow, A. J., Clayden, J. D., … Deary, I. J.: White matter integrity in the splenium of the corpus callosum is

related to successful cognitive aging and partly mediates the protective effect of an ancestral polymorphism in ADRB2. Behav. Genet., **40**, 146–156. (2010). doi:10.1007/s10519-009-9318-4

8. Dickie, D. A., Mikhael, S., Job, D. E., Wardlaw, J. M., Laidlaw, D. H., Bastin, M. E.: Permutation and parametric tests for effect sizes in voxel-based morphometry of gray matter volume in brain structural MRI. Magn. Reson. Imaging, **33**, 1299–1305. (2015). doi:10.1016/j.mri.2015.07.014
9. Deary, I. J., Gow, A. J., Taylor, M. D., Corley, J., Brett, C., Wilson, V., … Starr, J. M.: The Lothian Birth Cohort 1936: a study to examine influences on cognitive ageing from age 11 to age 70 and beyond. BMC Geriatr., **7**, 28. (2007). doi:10.1186/1471-2318-7-28
10. Jones, D. K., Williams, S. C. R., Gasston, D., Horsfield, M. A., Simmons, A., Howard, R.: Isotropic resolution diffusion tensor imaging with whole brain acquisition in a clinically acceptable time. Hum. Brain Mapp., **15**, 216–230. (2002). doi:10.1002/hbm.10018
11. Smith, S. M.: Fast robust automated brain extraction. Hum. Brain Mapp., **17**, 143–155. (2002). doi:10.1002/hbm.10062
12. Jenkinson, M., Smith, S.: A global optimisation method for robust affine registration of brain images. Med. Image Anal., **5**, 143–156. (2001).
13. Clayden, J. D., Muñoz Maniega, S., Storkey, A. J., King, M. D., Bastin, M. E., Clark, C. A.: TractoR : Magnetic Resonance Imaging and Tractography with R. J. Stat. Softw., **44**, 1–18. (2011).
14. Behrens, T. E. J., Berg, H. J., Jbabdi, S., Rushworth, M. F. S., Woolrich, M. W.: Probabilistic diffusion tractography with multiple fibre orientations: What can we gain? Neuroimage, **34**, 144–155. (2007). doi:10.1016/j.neuroimage.2006.09.018
15. Muñoz Maniega, S., Bastin, M. E., McIntosh, A. M., Lawrie, S. . M., Clayden, J. D.: Atlas-based reference tracts improve automatic white matter segmentation with neighbourhood tractography. In ISMRM 16th Sci. Meet. Exhib. (p. 3318). (2008).
16. Clayden, J. D., King, M. D., Clark, C. A.: Shape Modelling for Tract Selection. In Y. GZ., H. D., R. D., N. A., & T. C. (Eds.), Lect. Notes Comput. Sci. vol 5762 (pp. 150–157). Springer, Berlin, Heidelberg, (2009). doi:10.1007/978-3-642-04271-3_19
17. Hill, C. S., Clayden, J. D., Kitchen, N., Bull, J., Harkness, W., Clark, C. A.: A feasibility study of neighbourhood tractography in the presence of paediatric brain tumours. In Proc. Autumn Meet. Soc. Br. Neurol. Surg. (2009).